

GaAs buffer layer morphology and lateral distributions of InGaAs quantum dots

A. Roshko,^{a)} T. E. Harvey, S. Y. Lehman,^{b)} R. P. Mirin, K. A. Bertness, and B. L. Hyland
National Institute of Standards and Technology, Boulder, Colorado 80305

(Received 27 October 2004; accepted 7 March 2005; published 9 June 2005)

Atomic force microscopy was used to study the morphology of GaAs buffer layers and the density and height distributions of self-assembled InGaAs quantum dots (QDs) grown on these buffers by molecular-beam epitaxy. The surface roughness and terrace size of 500 nm thick buffers were found to be independent of substrate preparation technique, but did vary depending on whether the buffers were grown either continuously, with a pulsed start, or with a final anneal. A short anneal at the QD growth temperature increased both the size of the surface features and the height of mounds on the buffer grown with a pulsed start. The variations in dot distributions on these three buffer types were similar, indicating that the length of step edges does not determine the density of QDs. The standard deviation in dot density was found to vary from 16 to 28% of the average dot density across the central $26 \times 26 \text{ mm}^2$ region of the 5 cm wafers. The standard deviation in dot height was 10% or less of the average height. An inverse relationship was found between the dot height and density distributions, suggesting that a uniform amount of QD material was deposited on the wafers, but that the nucleation of the dots was nonuniform.

[DOI: 10.1116/1.1900729]

I. INTRODUCTION

Numerous devices that utilize quantum dots (QDs) because of their unique optical and/or electronic properties are under development. For production, the majority of these devices will require that the density and size of the dots be consistent or have controlled variations across the surfaces of wafers on which the devices are processed. Several studies have examined the wafer-to-wafer differences in QD density as a function of growth conditions.¹ However, the lateral distribution of dot density across the wafer surface has not been previously reported.

Studies have shown that substrate aging and pregrowth etching can cause substantial changes in buffer layer roughness.^{2,3} It has also been shown that different buffer growth conditions can lead to quite different surface morphologies, from step flow growth to mounding.⁴⁻⁹ It might be expected that these differences in buffer morphology would lead to differences in QD formation.

We describe here the influence of substrate preparation methods and buffer layer growth conditions on buffer layer roughness. We identify distinct buffer layer morphologies resulting from different growth conditions and examine the influence of these on QD distributions. We also describe the lateral variation in dot density and height across individual wafers. Although the buffer morphology was found to have no observable effect on the QD distribution, large variations were discovered in the lateral distribution of dots across individual wafers.

II. EXPERIMENTAL METHODS

Specimens were grown by molecular-beam epitaxy (MBE) on 5 cm (2 in.) diameter, Si-doped, $(100) \pm 0.03^\circ$ GaAs substrates. The MBE system has been described in detail elsewhere.¹⁰ The thickness variation across wafers grown in this system has been measured to be less than 0.05% /mm,¹⁰ and the temperature variation across the wafer is estimated to be 5 °C.

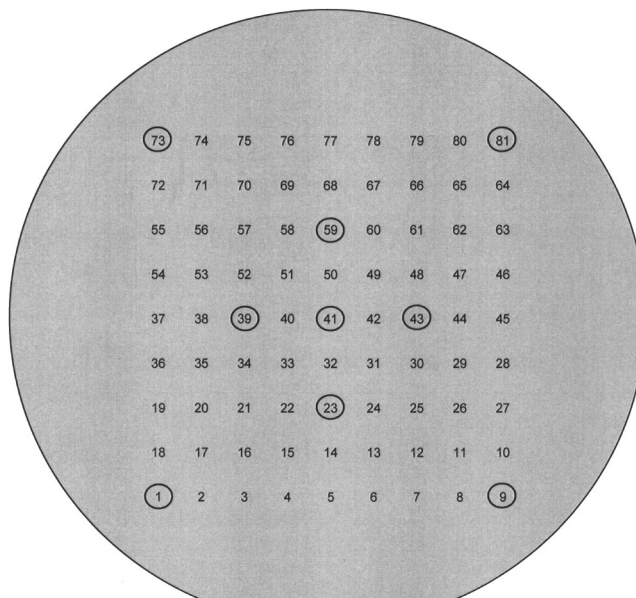


FIG. 1. Schematic showing the positions of the 81 analysis points used to generate maps of the QD density and height, relative to the edges and major flat on the wafers. The circled points are those analyzed on buffer layer samples to determine the sample rms roughness, R_q .

^{a)}Electronic mail: roshko@boulder.nist.gov

^{b)}Current address: College of Wooster, Wooster, OH.

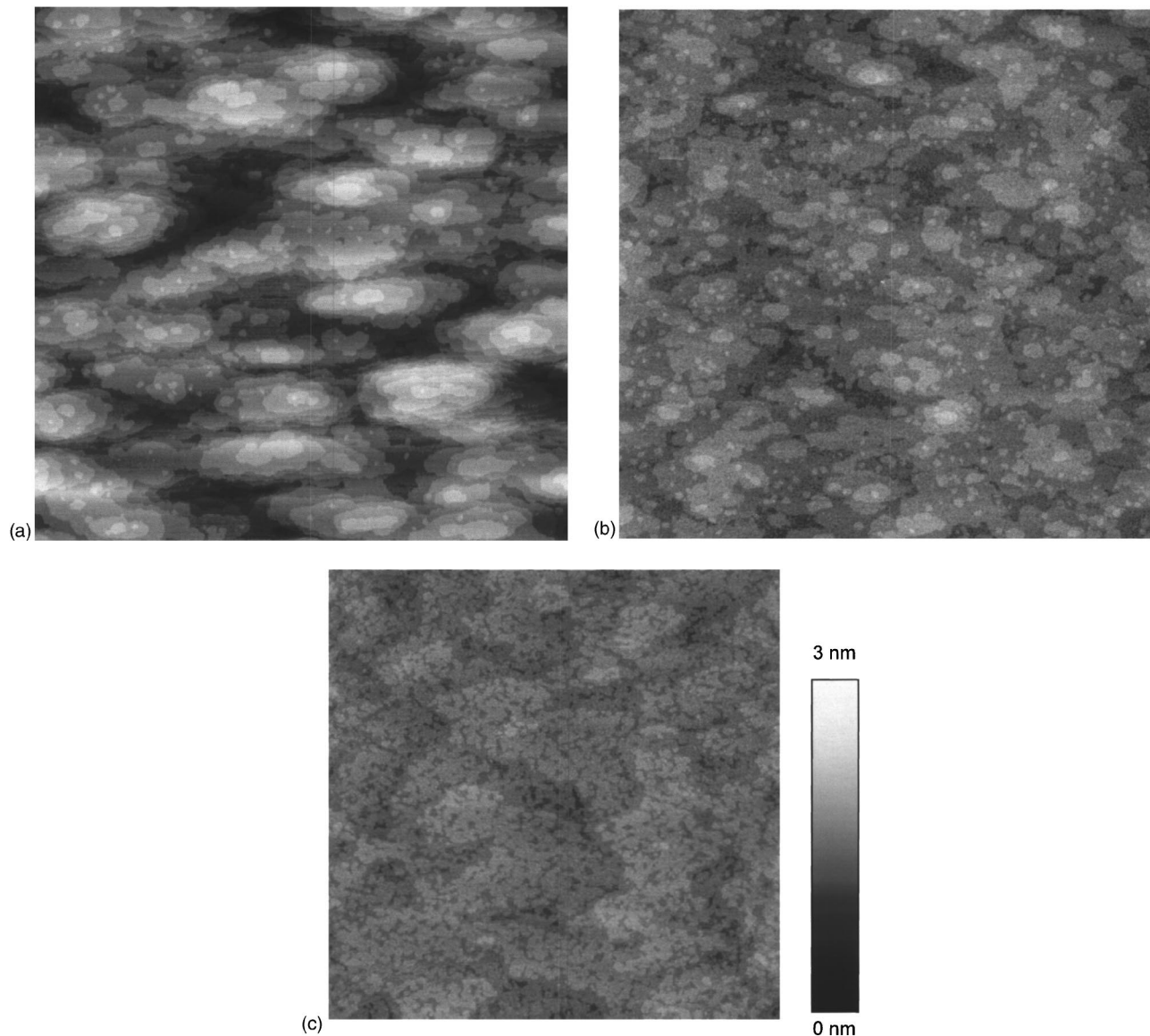


FIG. 2. AFM images of the three different buffer types studied: (a) pulsed start, (b) continuous, and (c) annealed. The images are all $3 \times 3 \mu\text{m}^2$.

Three different substrate preparation methods were examined: (1) “as-received” wafers had been stored for ~ 1 year in sealed epi-ready packages under ambient conditions; (2) “HCl etched” wafers were etched with a 1:1 mixture of HCl:H₂O for 1 min at room temperature and rinsed with flowing deionized water; (3) “PAW-HCl etched” wafers were etched with a 3:1:10 mixture of H₂O₂:NH₄OH:H₂O for 3 min at room temperature, then dipped in HCl and rinsed with deionized water. All of the wafers underwent thermal desorption of the oxide in the MBE chamber at 620 °C with an As beam equivalent pressure of 1.2×10^{-3} Pa (9×10^{-6} Torr). The substrate surface was monitored by reflection high-energy electron diffraction during desorption to confirm oxide removal.

GaAs buffer layers, 500 nm thick, were grown on the substrates with a deposition rate of $\sim 1 \mu\text{m}/\text{h}$. Three different types of buffer layer were examined: “pulsed start,” “continuous,” and “annealed.” For pulsed start buffers, the Ga

was deposited (with a continuous As overpressure) in cycles of increasing length separated by 10 s pauses, starting with a 1 s Ga cycle, for the initial 100 nm of growth. The remaining 400 nm were grown continuously. The initial temperature during growth of the pulsed start buffers was 620 °C; this was decreased to 600 °C by the time the continuous growth started. Continuous buffers were grown without pausing at 600 °C. Annealed buffers were deposited continuously at 600 °C and then annealed for 15 min at 600 °C.

Prior to QD growth, the samples were cooled further to 530 °C, under As overpressure, and held for 5 min to stabilize the temperature of the entire wafer. The dots were grown with alternating cycles of 0.25 monolayer (ML) In (at a rate of ~ 1.0 ML/s), As (5 s), 0.31 ML Ga (at a rate of ~ 0.3 ML/s), then As (5 s), for a total thickness of 2.5 ML. The wafer rotation speed during QD growth was 10 rpm. The nominal QD composition was $\text{In}_{0.44}\text{Ga}_{0.56}\text{As}$.

TABLE I. Buffer layer feature dimensions and step edge line intercepts.

	As grown		After hold at 530 °C		After hold at 530 °C		Average
	Feature dimensions (nm)		Feature dimensions (nm)		Line intercepts (μm)		
Buffer type	Along $[0\bar{1}1]$	Along $[01\bar{1}]$	Along $[0\bar{1}1]$	Along $[01\bar{1}]$	$[01\bar{1}]$ line	$[0\bar{1}1]$ line	
Pulsed	690 ± 210	250 ± 60	1030 ± 210	390 ± 70	16.1 ± 0.1	7.9 ± 0.1	12.0
Continuous	170 ± 40	80 ± 20	220 ± 50	130 ± 20	8.8 ± 0.2	6.3 ± 0.2	7.6
Annealed	30 ± 11	30 ± 10	60 ± 100	70 ± 10	13.3 ± 0.3	12.7 ± 0.3	13.0

The buffer layer morphology and roughness, and the QD density and height were measured using atomic force microscopy (AFM). Imaging was performed under ambient conditions with commercial pyramidal Si tips in tapping mode. Each QD specimen was analyzed by taking measurements at an array of 81 points (see Fig. 1) which covered the central $26\times 26\text{ nm}^2$ region of the wafer. The corners of the array are 7 mm from the wafer edge, and the centers of the array sides are 12.4 mm from the wafer edge. A scan size of $3\ \mu\text{m}$ was used to eliminate the effect of small-scale local variations. Buffer layers were also measured with $3\ \mu\text{m}$ scans at an array of nine points; these points are circled in Fig. 1.

For the buffer layer analysis, the root-mean-square (rms) roughness, R_q , of the AFM images was determined for each of the nine images and these values were averaged ($R_q = [(\sum z_i - z_{\text{avg}})^2/n]^{1/2}$, where z_i is the height of each pixel and n is the number of pixels). The number of times the buffer step edges intercept an equally spaced grid of ten lines—five horizontal and five vertical—placed on the images was measured to give an indication of the step edge length. The QD images were analyzed with a computer program which identified the dot positions by finding local maxima. The program generates an image with crosses at the dot positions found; the accuracy of the program was verified by visual inspection of these positions. The dot heights were determined by finding the average background level for the image and subtracting it from the height at each of the maxima identified.

III. RESULTS AND DISCUSSION

The three different substrate preparation techniques resulted in quite different surface morphologies after oxide desorption, with R_q s of 0.5, 1.0, and 1.3 nm for the HCl etched, as-received, and PAW-HCl etched wafers, respectively. After 500 nm of buffer growth, there were no obvious morphological differences between wafers with the three different substrate preparations, and the R_q s were nearly identical, ranging from 0.2 to 0.3 nm. These results differ from those found previously for buffers grown by organometallic vapor phase epitaxy (Ref. 3) and will be discussed in more detail elsewhere.¹¹

Distinct morphologies were found for the pulsed start, continuous, and annealed buffers, as shown in Fig. 2. The buffers grown by initially pulsing the Ga are mounded [Fig. 2(a)]. The mounds are elongated along the $[0\bar{1}1]$ direction

(Table I). Mounds have been observed under a variety of growth conditions for GaAs (001) homoepitaxy,^{5–7,12} and have been proposed to result from an unstable growth mode due to the presence of a barrier at step edges (Schwoebel barrier¹³ or diffusion bias¹⁴) that inhibits the movement of adatoms off a terrace. The influence of this step edge barrier can be diminished by decreasing the adatom diffusivity.^{7,15} In the mounded samples studied here, the pause between Ga pulses—during the early stages of the buffer growth—allowed the Ga to diffuse further on the surface, giving an increased diffusion length. This would increase the effect of the step edge barrier and promote the formation of mounds. Once the mounds formed, they persisted throughout the buffer growth—even when the growth rate was increased by switching to continuous deposition—giving an effectively shorter diffusion length. Mounds have also been proposed to be the incompletely smoothed remnants of the initial substrate surface, and have been modeled with an anisotropic nonlinear Kardar–Parisi–Zhang equation.^{8,9,14}

As shown in Fig. 2(b), the continuous buffer layer deposition did not cause mounding in samples without the initial pauses between Ga pulses. The terraces on the continuously grown samples are elongated along $[0\bar{1}1]$ (Table I), as are the mounds on the pulsed start buffers, indicating anisotropy in the diffusion coefficients or sticking probabilities along the $[0\bar{1}1]$ and $[01\bar{1}]$ directions.⁴ These buffers are substantially smoother than the pulsed start buffers; their rms roughness values were approximately one-half of those of the pulsed start buffers (Table II). Their average feature size is also smaller (Table I).

The annealed buffers have large incompletely filled terraces [Fig. 2(c)]. These are similar to the two-dimensional ML islands and holes previously observed on GaAs (100) buffers that had been annealed for 1 h at 600 °C and quenched.¹⁶ The sizes of the islands and holes observed in this study are significantly larger than those described previously, probably because the samples in this study were cooled relatively slowly compared with the 2 s quench used in that study.¹⁶

As already described, the substrates were cooled to the growth temperature and held for 5 min prior to QD growth. These extra steps are similar to annealing, but at a lower temperature. To determine the influence of these additional steps on the buffer morphology, specimens of each buffer type were imaged after undergoing the hold at 530 °C (Fig.

TABLE II. Buffer layer roughness, R_q (nm)

Specimen set	Pulsed start	Continuous	Annealed
A	0.42	0.27	0.17
B	0.47	0.19	0.18
C ^a	0.52	0.20	0.17
D	0.30		
Average	0.43	0.22	0.17
Standard deviation	0.09	0.04	0.01

^aThe C specimens were cooled to 530 °C and held for 5 min before cooling.

3). This low-temperature anneal did not substantially change the buffer morphology; the pulsed start buffers still have mounds, and both the continuous and annealed buffers are still relatively smooth. The mound height and lateral dimensions on the pulsed start buffers increased slightly after the 530 °C hold (Table I and results for Sample “C” in Table II). Likewise, the average island size on the continuous and annealed buffers increased after the 5 min anneal (Table I); however, their surface roughness did not (Table II). These changes may be the result of a variety of effects, either kinetic, thermodynamic, or both. Interestingly, on the continuous buffer after the 5 min anneal, there appear to be small islands or hillocks at the edges of the larger islands [Fig. 3(b)]. These may result from the step edge barrier, which may be larger at the lower anneal temperature, and may warrant further investigation.

The average number of step edge intercepts along the length of a line was measured for the buffers held 5 min at 530 °C (Table I). The anisotropy in feature dimensions on the buffers is reflected in the step edge intercepts. As expected, there are more intercepts along lines parallel to the short dimensions of the surface features. The number of step edge intercepts is smallest for the continuously grown buffer, consistent with this specimen having a low rms roughness and relatively large feature size. The pulsed start and annealed buffers—which have, respectively, a very rough surface and very small feature sizes—have substantially higher numbers of intercepts (by <50%), indicating a greater step edge length on these two samples than on the continuous buffer.

AFM images of the QDs grown on the three different buffer types, taken at the center of each wafer, are also shown in Fig. 3. From these images, it can be seen that the size and density of the dots are qualitatively similar in the three different samples. Contour plots of the QD densities on the wafers (Fig. 4), however, show substantial variations across each wafer. For all three specimens, there is an area of the wafer where the dot density is twice that in another region. The wafer-to-wafer change in average density and height, however, is small (Table III) and less than the standard deviation within each wafer.

Thus, there was no obvious influence of the buffer layer morphology on the QD distribution, and the large lateral variations in dot distributions across wafers are not due to local variations in buffer morphology.

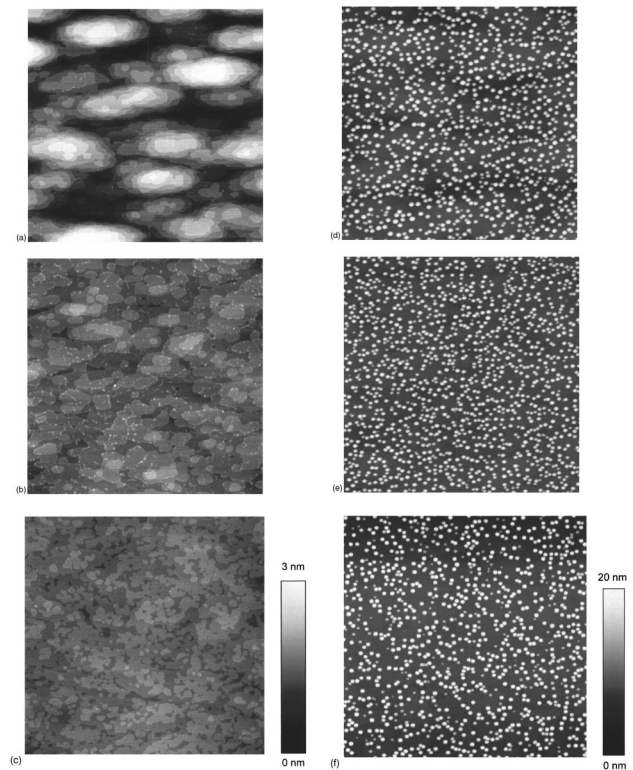


FIG. 3. AFM images of substrates with the three different buffer types, which have undergone an additional cooling to and 5 min hold at 530 °C: (a) pulsed start, (b) continuous, and (c) annealed. AFM images from the center of each wafer with QDs grown on the three different types of buffer: (d) pulsed start, (e) continuous, and (f) annealed. The images are all $3 \times 3 \mu\text{m}^2$.

It is noteworthy that the specimens with the pulsed start and annealed buffers, which have substantially more step edge length than the continuous buffer, as indicated by the line intercept measurements (Table I), have smaller average dot densities than the continuous buffer sample. This indicates that factors other than the step edge length determine the density of dots. From the AFM image [Fig. 3(d)], it can be seen that the dots on mounded buffers do not appear to be aligned with terrace edges.

The dot heights on the three wafers are more uniform than the dot densities (Fig. 4) and, again, the difference between wafers is small (Table III). The standard deviation in the dot height across each wafer is 10% or less of the average height, compared with the density for which the standard deviations range from 16 to 28% of the average (Table III). There is an inverse relationship between the dot height and density distributions for each wafer, as can be seen in Fig. 4, suggesting that the volume of material in the QDs is uniformly distributed, but that the dot nucleation was not. Potential sources of nonuniform nucleation are temperature gradients and nonuniform material distribution at the time of nucleation. Further work to investigate these possibilities is underway.

To check whether the volume of material in the dots was deposited uniformly, the product of the dot density and the height cubed (Dxh^3) was evaluated across the wafers. The parameter Dxh^3 is proportional to the average volume of

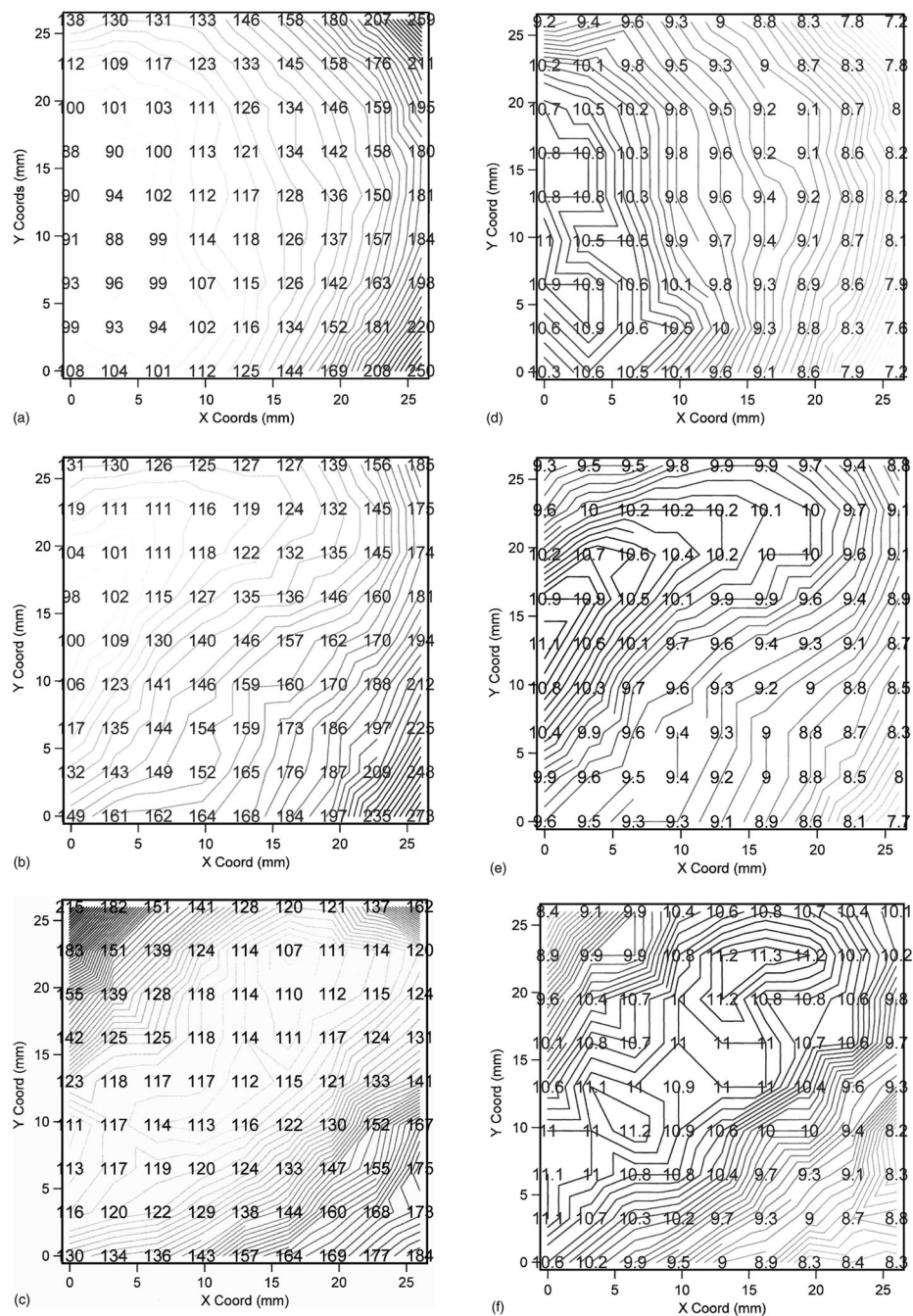


FIG. 4. Contour plots of the QD density (dots/ μm^2) on the three different buffers: (a) pulsed start, (b) continuous, and (c) annealed, and of the QD height (nm): (d) pulsed start, (e) continuous, and (f) annealed.

material in the dots per unit area or average thickness of the QD layer. Both Dxh^3 and the standard deviation for each wafer are given in Table III. For two of the specimens, pulsed start and continuous, the volume of material is more uniform across the wafer than either the density or height. For the pulsed start sample, the maximum variation in dot density and height are 194 and 53%, respectively, while the maximum variation in the “volume” per unit area is 31%. Likewise, for the continuous specimen, the maximum variations of 177 and 44% for the density and height are reduced

to 30% for the volume per unit area. For the annealed wafer, the variation in volume per unit area is quite large.

It is important to note that the volume approximation used here assumes that the shape of the dots does not change within a wafer. Transmission electron microscopy measurements have shown that the shape of InGaAs dots varies substantially, from pyramidal to multifaceted, for dots between 8.5 and 13 nm tall.¹⁷ This change in shape would have a significant effect on the volume of the dots. For the annealed specimen, which has the largest average dot height, 10.2 nm,

TABLE III. Average quantum dot density, height and Dxh^3 .

Buffer type	Density ($/\mu\text{m}^2$)		Height (nm)		Dxh^3 (nm)	
	Average	Standard deviation	Average	Standard deviation	Average	Standard deviation
Pulsed	135	38	9.4	0.9	0.108	0.007
Continuous	151	35	9.6	0.7	0.128	0.006
Annealed	134	22	10.2	0.9	0.140	0.020

the relatively large variation in dot volume across the wafer may be due to locally varying dot shapes. Shape changes may also contribute to the smaller variations in volume found for the other two samples.

It is interesting to speculate on the implications of these results for optical device processing. The maximum deviations in the dot height across the central $2.6 \times 2.6 \text{mm}^2$ region of the wafers are between 40 and 50%. Using a height cubed estimate for dot volume, this translates into a volume change of $\sim 275\%$ and a predicted shift in peak wavelength response of $\sim 100 \text{meV}$.¹⁸ In addition, assuming that nonradiative processes are minimized to the point where device saturation is possible, the large variations in QD density, from 100 to 200% maximum in the central $2.6 \times 2.6 \text{mm}^2$ square of the wafers studied, would cause similarly large variations in the sensitivity or brightness of devices from different regions of the same wafer.

IV. SUMMARY

Three distinct buffer morphologies, with varying degrees of surface roughness, were identified for buffers grown continuously, with a pulsed start and with a postgrowth anneal. The surface features are consistent with growth models that assume a step edge barrier or diffusion anisotropy. A short anneal at the lower QD growth temperature was found to cause an increase in the size of the surface features, but little change in the surface roughness. Some increase in roughness was observed in the mounded buffer after annealing.

Dots were grown on these three buffer types, and their density and height distributions were analyzed. The variations in dot distributions on different buffer types were found to be similar, indicating that the buffer roughness and step edge length do not determine the dot distribution across wafers. The standard deviation in the dot density across individual wafers was large, 16 to 28% of the average, while the

standard deviations in dot height were smaller, 10% or less of the average. An inverse relationship between the dot height and density distributions was found, suggesting that the total amount of QD material deposited was uniform, although the QD nucleation was not.

- ¹See, e.g., G. S. Solomon, J. A. Trezza, and J. S. Harris, *Appl. Phys. Lett.* **66**, 3161 (1995); H. Li, Q. Zhuang, Z. Wang, and T. Daniels-Race, *J. Appl. Phys.* **87**, 188 (2000); F. Patella, M. Fantoni, F. Arciprete, S. Nuffris, E. Placidi, and A. Balzarotti, *Appl. Phys. Lett.* **78**, 320 (2001); T. J. Krzyzewski, P. B. Joyce, G. R. Bell, and T. S. Jones, *Phys. Rev. B* **66**, 201302 (2002); O. Suekane, S. Hasegawa, M. Takata, T. Okui and H. Nakashima, *Mater. Sci. Eng., B* **88**, 158 (2002).
- ²D. A. Allwood, S. Cox, N. J. Mason, R. Palmer, R. Young, and P. J. Walker, *Thin Solid Films* **412**, 76 (2002).
- ³D. A. Allwood, N. J. Mason, A. Mowbray, and R. Palmer, *J. Cryst. Growth* **248**, 108 (2003).
- ⁴E. J. Heller and M. G. Legally, *Appl. Phys. Lett.* **60**, 2675 (1992).
- ⁵C. Orme, M. D. Johnson, J. L. Sudijono, K. T. Leung, and B. G. Orr, *Appl. Phys. Lett.* **64**, 860 (1994).
- ⁶M. D. Johnson, C. Orme, A. W. Hunt, D. Graff, J. Sudijono, L. M. Sander, and B. G. Orr, *Phys. Rev. Lett.* **72**, 116 (1994).
- ⁷G. Apostolopoulos, J. Herfort, L. Däweritz, and K. H. Ploog, *Phys. Rev. Lett.* **84**, 3358 (2000).
- ⁸A. Ballestad, B. J. Ruck, M. Adamcyk, T. Pinnington, and T. Tiedje, *Phys. Rev. Lett.* **86**, 2377 (2001).
- ⁹A. Ballestad, B. J. Ruck, J. H. Schmid, M. Adamcyk, E. Nodwell, C. Nicoll, and T. Tiedje, *Phys. Rev. B* **65**, 205302 (2002).
- ¹⁰T. E. Harvey, K. A. Bertness, R. K. Hickernell, C. M. Wang, and J. D. Splett, *J. Cryst. Growth* **251**, 73 (2003).
- ¹¹S. Y. Lehman, A. Roshko, R. P. Mirin, K. A. Bertness, and K. Cobry (unpublished).
- ¹²G. W. Smith, A. J. Pidduck, C. R. Whitehouse, J. L. Ghasper, and J. Spowart, *J. Cryst. Growth* **127**, 966 (1993).
- ¹³R. L. Schwoebel and E. J. Shipsey, *J. Appl. Phys.* **37**, 3682 (1966).
- ¹⁴J. Villian, *J. Phys. I* **1**, 19 (1991).
- ¹⁵R. Kunkel, B. Poelsema, L. K. Verheij, and G. Comsa, *Phys. Rev. Lett.* **65**, 733 (1990).
- ¹⁶M. D. Johnson, K. T. Leung, A. Birch, and B. G. Orr, *J. Cryst. Growth* **174**, 572 (1997).
- ¹⁷S. Y. Lehman, A. Roshko, R. P. Mirin, and J. E. Bonevich, *Mater. Res. Soc. Symp. Proc.* **737**, E13.40 (2003).
- ¹⁸C. Pryor, *Phys. Rev. B* **60**, 2869 (1999).